Potential of a virtual reality environment based on very-high-resolution satellite imagery for structural geology measurements of lava flows

Marion Jaud, Laurent Geoffroy, François Chauvet, Erwan Durand, François Civet

▶ **To cite this version:**

Marion Jaud, Laurent Geoffroy, François Chauvet, Erwan Durand, François Civet. Potential of a virtual reality environment based on very-high-resolution satellite imagery for structural geology measurements of lava flows. Journal of Structural Geology, 2022, 158, 10.1016/j.jsg.2022.104569 . insu-03684624

HAL Id: insu-03684624

https://insu.hal.science/insu-03684624v1

Submitted on 18 May 2024

HAL is a multi-disciplinary open access archive for the deposit and dissemination of scientific research documents, whether they are published or not. The documents may come from teaching and research institutions in France or abroad, or from public or private research centers.

L'archive ouverte pluridisciplinaire **HAL**, est destinée au dépôt et à la diffusion de documents scientifiques de niveau recherche, publiés ou non, émanant des établissements d'enseignement et de recherche français ou étrangers, des laboratoires publics ou privés.

Journal of Structural Geology
May 2022, Volume 158 Pages 104569 (10p.)
https://doi.org/10.1016/j.jsg.2022.104569
https://archimer.ifremer.fr/doc/00766/87832/

Archimer
https://archimer.ifremer.fr

Potential of a virtual reality environment based on very-high-resolution satellite imagery for structural geology measurements of lava flows

Jaud Marion [1, 2, *], Geoffroy Laurent [2], Chauvet François [2], Durand Erwan [2], Civet François [3]

[1] Univ. Brest, IUEM, CNRS, UMS 3113, Pôle Image et Instrumentation, Technopôle Brest-Iroise, Rue Dumont d'Urville, Plouzané, 29280, France
[2] Univ. Brest, IUEM, UMR 6538, Géosciences Océan, Technopôle Brest-Iroise, Rue Dumont d'Urville, Plouzané, 29280, France
[3] SAS VR2Planets, 2 chemin de la Houssinière, 44322, Nantes Cedex 3, France

* Corresponding author : Marion Jaud, email address : marion.jaud@univ-brest.fr

Abstract :

Combining very-high-spatial resolution (<1 m) and the ability to provide stereo-pairs for 3D topographic reconstructions, Pleiades satellites offer great potential for large-scale and high-resolution studies in geosciences. In parallel, research-dedicated Virtual Reality (VR) applications are emerging based on high-quality data. We examined the potential of a VR application derived from very-high-resolution Pleiades imagery to infer the orientation of individual flows from kilometers-thick lava piles in the eastern Afar rift area (Stratoïd Formation, Djibouti). Based on Pleiades Digital Elevation Models and orthoimages, we compared two approaches: i) a "classical" method in "Mouse Mode" and ii) a method using the VR application. Both methods provide similar results in facet orientation measurements over the studied transects. Nevertheless, VR enables operator immersion in a very realistic virtual environment combining aerial synoptic and ground-level views. Our studied case shows the potential of those methods to get high-quality and unexpected structural information from an otherwise inaccessible environment.

Highlights

► 3D stereo-reconstruction of the Asal-Ghoubbet rift from Pleiades satellite imagery. ► Virtual environment derived from high-resolution Pleiades DEM and orthoimage. ► Quality control on virtual structural geology exploration and measurements. ► Large-scale virtual geological exploration.

Keywords : Pleiades satellite imagery, Virtual reality, High resolution DEM, Geological structure 3D orientation, Dip and dip direction measurement, Asal-ghoubbet rift

Please note that this is an author-produced PDF of an article accepted for publication following peer review. The definitive publisher-authenticated version is available on the publisher Web site.

1. Introduction

To analyze the structure of a fault network, a pile of lava flows or of sedimentary strata; the structural geologist has to perform numerous orientation measurements, using a field compass. However, some outcrops can be inaccessible to direct measurement, particularly in steep terrain. Furthermore, as the orientation is measured using the compass box, in situ measurements are biased by local roughness effects. This is especially the case for lava flows, making any compass measurement subject to large errors. In addition, magnetic remanence from rocks containing ferromagnetic minerals, such as basalts, may strongly alter the reliability of compass

measurements (Riisager et al., 2003).
3D models derived from aerial or terrestrial remote sensing data can be used to avoid those biases and obtain a large amount of structural data on inaccessible outcrops. This approach was use to analyze the 3D architecture of the volcanic traps through the North Atlantic Igneous Province. Pedersen et al. (1997) combined aerial photogrammetry and field work to generate a three-dimensional (3D) reconstruction of the traps stratigraphy along the East Greenland volcanic margin. In the West Greenland Volcanic Province, Riisager et al. (2003) relied on helicopter stereo-photogrammetry to extract dip/strike of lava flows and correct their paleomagnetic data from the tectonic tilt. Nelson et al. (2011) used Terrestrial Laser Scanning (TLS) to generate 3D point clouds and extract structural characteristics of lava flow sequences, sedimentary units, dykes and lava tubes.

With the improvement of remote sensing methods over the last few decades, Digital Elevation Models (DEMs) of high spatial resolution now make it possible to capture the small-scale topographic roughness. Moreover, satellite observations are suited to regional studies, allowing large-scale coverage, repetitive coverage and minimization of the amount of work needing to be done in the field. Furthermore, satellite remote sensing makes it possible to gather data over inhospitable areas where field work is challenging. These data can be used to constrain geologic structures in three dimensions and obtain surface bedding measurements. Most of studies of this kind are based on ASTER, Landsat TM or SPOT images (e.g. Nishidai and Berry, 1990; Massironi et al., 1997; Bilotti et al., 2000). However, until recently, the spatial resolution of these satellite images prevented the study of small-scale features. The new generations of very-high-resolution (< 1 m) satellites, *WorldView*, *GeoEye* or, as in this study, *Pleiades*, offer a greater potential to combine large scale and very high spatial resolution studies (Poli et al., 2015; Collin et al., 2018). Moreover, due to the platform agility and short revisit time, these satellites can provide stereo pairs for 3D topographic reconstructions, providing new opportunities for geoscience applications (Berthier et al., 2014; Zhou et al., 2015; Bagnardi et al., 2016; Letortu et al., 2020). With this very-high-resolution stereo-imagery, the surface topography can be reconstructed with a precision of a few decimetres (Zhou et al., 2015). To our knowledge, very-high-resolution satellite DEM and orthoimages have never been used for structural analysis of layered sequences such as lavas. For the specific problem of lava sequences, the resolution of this new generation of satellites is sufficient to detect the flow boundaries.

In parallel, over the last decade, Virtual Reality (VR) solutions have become more accessible, offering new tools for geoscience. Among these “virtual worlds”, high-immersive VR emerged with the development of devices that surround the user in large 3D viewing areas (Checa and Bustillo, 2020). Facilitating a visual understanding of complex concepts and environments, these tools are already used for educational purposes (Moysey and Lazar, 2019; Chenrai and Jitmahantakul, 2019). Moreover, VR applications are now emerging dedicated to research purposes and based on high-quality data (Civet and Le Mouélic, 2015; Le Mouélic et al., 2018). The VR application used in this study is not only a visualization tool, but also an immersive

environment to carry out structural measurements.

In this contribution, we apply a new methodology based on high resolution DEMs to identify and provide full and accurate orientations of sequences of hundreds of basalt lava flows outcropping along steep relief. The method measures surfaces up to several hundreds or thousands of square metres. In this way, the natural roughness and the complex topography inherent to the lava flows are smoothed on a mean 3D plane.

We show the potential of the use of very high spatial resolution Pleiades satellite imagery for structural geology exploration and measurements, and demonstrate how to perform such geological measurements in a VR environment created from the Pleiades DEMs and orthoimages. The objective of the paper is not to extend on the structural meaning of the results but to evaluate the applicability of such methods to the studied case, and demonstrate their potential for other similar analyses.

2. Description of the studied area

We applied our method to the Asal rift in Djibouti (Figure 1a), which is part of the active and segmented plate boundary between the Arabia and Somalia/Nubia plates (Manighetti et al., 1998; Cattin et al., 2005; Doubre et al., 2007). Apart from Neogene sediments in the hanging walls of normal faults, the geological formations are made of superposed lava flows, mainly of basaltic composition. Most of the observable tectonic features in Djibouti result from a late-stage extensional strain that affected the upper-Stratoïd basaltic lava formation (~2-1 Ma, Lahitte et al., 2003; thickness less than 150m - Manighetti et al., 1998; Geoffroy et al., 2014). Recent studies that compile observations in the field and those made using Google Earth suggest that the underlying volcanic sequences could form fan-like syn-extensional wedges unconformably overlain by the Upper Stratoïd basalts (Geoffroy et al., 2014). These volcanic wedges resemble Seaward Dipping Reflector sequences that are characteristic of volcanic-type passive margins (e.g., Geoffroy, 2005). The information about the dominant tectonics in SE Afar must therefore be sought in the overall structure of the upper-crustal lava piles located beneath the Upper Stratoïd Formation (Figure 1b, 1c, 1d). Those formations, namely the Lower Stratoïd (~3.3 to 2 Ma, Lahitte et al., 2003; Kidane et al., 2003) and Dahla formations (8.5 to 3.6 Ma) (Gasse et al., 1987; Le Gall et al., 2015); locally outcrop in the Asal area in SE Afar in specific eroded areas and along the footwall of the main recent normal faults.

In syn-extensional wedges, sedimentary strata or lava flows decrease in dip with time. They also may vary in strike with time according to stress reorganization and the rift evolution. The aim of our study was to succeed in capturing the continuous variations in orientation (strike and dip) of basaltic flows within a thick volcanic pile beneath the Upper Stratoïd Formation regarding its vertical section, an as yet unreached goal in volcano tectonics. The study area for these tests covers 1000 km² (Figure 1a) and includes altitudes varying from -150 m to 1730 m and steep slopes (around 50% for the steepest).

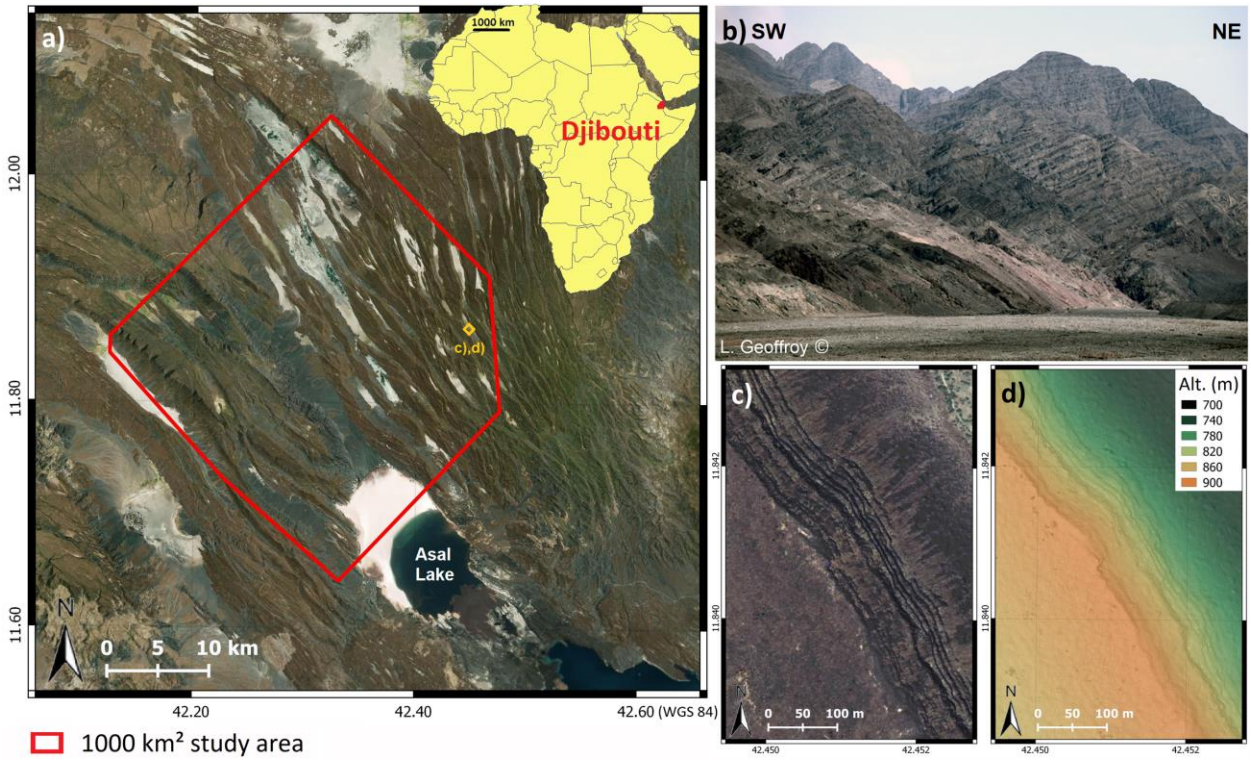

Figure 1. a) Location of the study area, along the Asal-Ghoubbet rift (Djibouti), to the north of Lake Assal. The red polygon depicts the 1000 km² study area covered by Pleiades satellite images. b) Photograph of SW-ward tilted pile of lava flows in the Doubié valley NW of the Asal Lake. Each lava flow is several meters thick. Individual lava flows are visible both on the orthoimage (c) and in topographic variations in the DEM (d) computed from the Pleiades stereo pairs (images provided by CNES 2019 - Distribution Airbus DS).

3. Data acquisition and processing

3.1. Pleiades DEM and orthoimage

The Pleiades satellite constellation is composed of two agile optical imagery satellites (1A and 1B) controlled by *CNES* (National Centre for Space Studies, French government space agency) and *Airbus Defence and Space*. Pleiades satellites are designed for a range of very-high-resolution (VHR) remote sensing applications. In particular, because of their high agility in roll, pitch and yaw, they offer along-track stereo or tri-stereo acquisition capability.

The images were collected between 9 November 2018 and 25 December 2018. They were acquired in multi-view stereo mode, covering a 1000 km² study area, with a B/H ratio between 0.25 and 0.30 (suited to areas of mountainous relief). The stereo-pairs were processed with ASP® (Ames Stereo Pipeline - Beyer et al., 2018; Shean et al., 2016), NASA's Open Source Automated

Stereogrammetry Software. From the computed 3D point cloud, a DEM and an orthoimage were computed (Figures 1c and 1d). To keep the highest possible resolution on the orthoimage, they were extracted with a spatial resolution of 50 cm. To facilitate the measurements in the reconstructed 3D environment, the results were projected in UTM coordinates (UTM 38N).

3.2. Method for lava flow orientation measurements

CloudCompare® is an open-source 3D software for point cloud processing allowing 3D visualization and point picking (Figure 2c). Due to the volume of data (26 GB for the whole area), *CloudCompare*® cannot handle displaying, moving and point picking over the whole area. Three transects (of about 500 m wide and 2 km long, approximately 150 MB per transect) were therefore selected along the rift axis to facilitate data manipulation (Figure 2a). The limits of the lava flows were manually picked, to extract the orientation (also decomposed into dip and dip direction) of the lava flows as a function of the altitude.

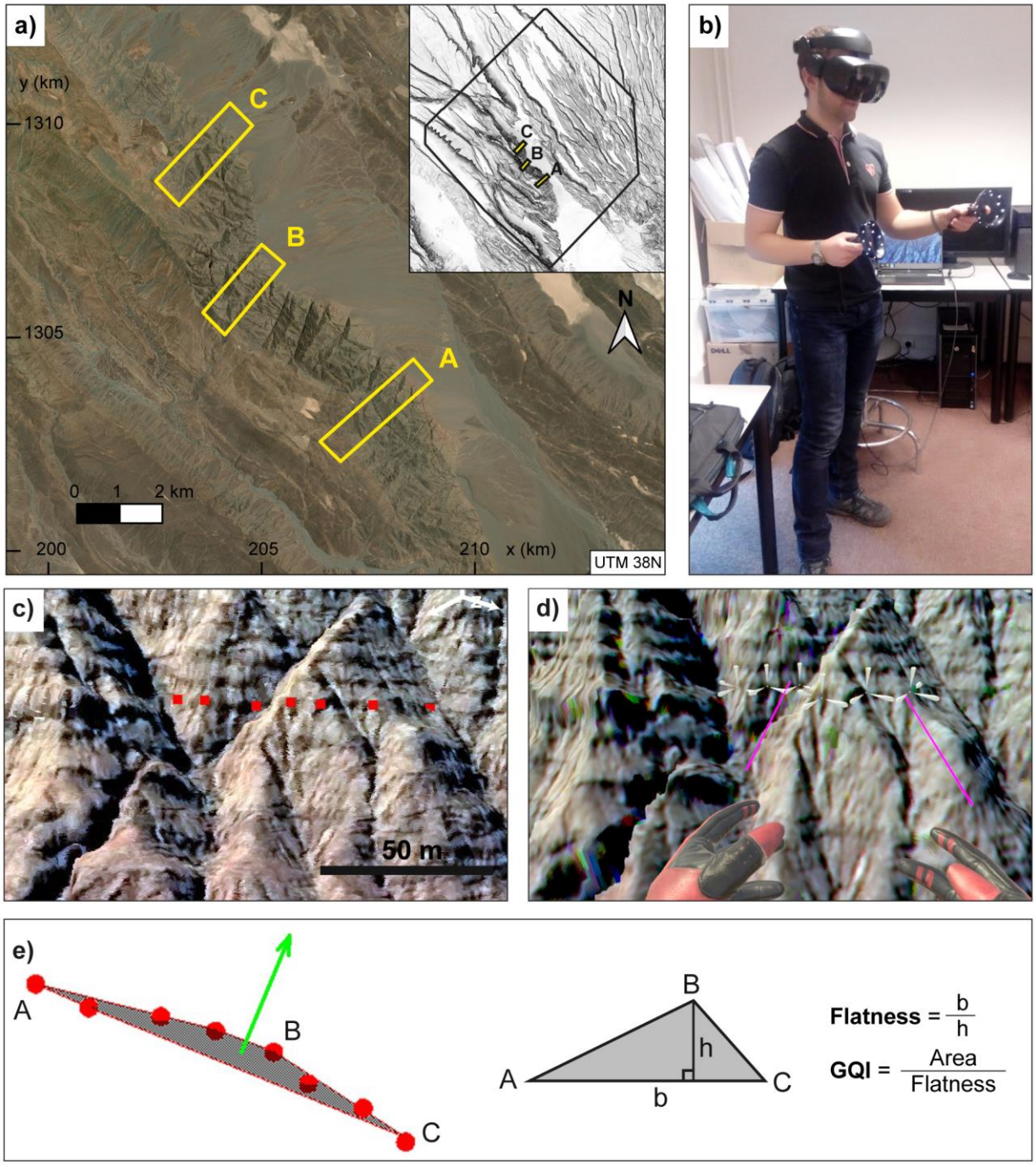

Figure 2. a) Location of the transects defined along the Asal Rift in QGIS® in order to crop the orthoimage and the DEM before being loaded in *CloudCompare*® (background image provided by BingSat®). b) User with Oculus Rift headset and two controllers digitizing the volcanic flow boundary in the VR application. c) "Mouse Mode" point picking (red squares) along a volcanic flow limit in *CloudCompare*®. d) VR point picking along the same volcanic flow limit than in c), in 2.5D mode (i.e. the point is automatically pinned against the DEM surface). e) Fitting plane facet and its normal vector computed from the picked points (red dots) using the *Matlab*® routine.

The resulting triangle (ABC) is then characterized geometrically (flatness and GQI ratio, see text for explanations).

A Virtual Reality (VR) environment (Figure 2b and 2d) was developed by a subcontractor (*VR2Planets*© http://vr2planets.com) specialized in planetary data integration into virtual environments. This proprietary software was designed to run on a laptop using a powerful graphic card (Nvidia GeForce RTX 2070) equipped with a Windows Mixed Reality headset (Samsung Odyssey+). To create the virtual world, a graphic engine (*Unity3D*®) was used to load the data and render the experience. Each pixel of the DTM was integrated and processed to generate a mesh textured with the orthoimages. To preserve the scientific integrity of the data and the fluidity of the application, some rendering optimization was implemented (*VR2Planets*©). These optimizations, based on quadtree methods and shader algorithms (Cozzi and Ring, 2011), make it possible to load a vast amount of data at full resolution in a georeferenced world, keeping each pixel of the DTM and of the orthoimage. Furthermore, classical geological tools were integrated into the application *VR2Planets*©. In particular, a pointer was used in this study for point picking. For comparison with Cloud Compare, point picking in the VR application is done on the same transects as in "Mouse Mode" (MM).

In order for the method to be as consistent as possible between MM and VR, a raw point list of the picked (X, Y, Z) coordinates was exported for each volcanic flow both in MM and in VR approaches. The same *Matlab*® routine was applied to both datasets to fit a plane facet to each list of picked points (Figure 2e). The facet was defined as a linear polynomial surface of degree 1 and the fitting method, implemented through the *fit* function, was a linear least-square method. The points were preferably picked in the neighborhood of topographic edges or concavities to minimize facet flattening and so optimize the significance of the facet orientation. For each facet, the *fit* function allowed to export its centroid coordinates, normal vector, dip and dip direction.

3.3. Quality control of digitized facets

The quality of the resulting orientation measurements is impacted both by the resolution and accuracy of the DEM and orthoimage and by the quality of the digitization of the facets corresponding to the lava flows.

3.3.1 – Quality of the 3D model

About the quality of the 3D model, earlier studies have reported that sub-meter accuracy is obtainable for Pleiade DEMs (Zhou et al., 2015; Stumpf et al., 2014; Perko et al., 2014). As no topographic reference data at VHR were available on our study area to assess the accuracy, a first-order assessment of the topographic reconstruction was made by comparing our DEMs to the ALOS DEM at 30 m resolution. Then, we took advantage of the overlapping zones between the various Pleiades stereo-pairs. On each overlapping zone, the DEMs were compared two by two. We obtained a mean error of 0.81 m, with a standard deviation of 5.76 m that was mainly due to

local artefacts caused by false correlation (because of shadows, saturation on highly reflective soils or clouds). It is noteworthy this error is not a function of altitude and the reconstruction of lava sequences remains relatively consistent, which excludes a major impact of the DEM quality on the interpretation of the digitized facet characteristics.

3.3.2 – Quality of facet digitizing

Another possible source of error is related to the relevance and precision of facet digitizing. The relevance of the choice of digitized facets is partly linked to the operator's geological experience (choice of significant facets for structural analysis, away from faults, etc.), but also to geometric criteria. We define a Geometric Quality Index (GQI). From the digitized points, the facet is assimilated to a triangle to the first order, with the two furthest points defining the base of the triangle and the furthest point from this base defining the triangle height (Fig. 2e). The “flatness” of the triangle is defined as the ratio of the base to the height (thus, this index will be high for a "flattened" triangle). The GQI is defined as the ratio of the area of the triangle to the flatness index (Eq. 1).

$$GQI = \frac{Area}{Flatness} \qquad \text{(Eq. 1)}$$

GQI will therefore be high for a facet with a large surface area and little flatness. The higher the GQI, the more geometrically favorable the facet. To empirically define a threshold for GQI, nested facets were defined on the same lava flow (Figures 3a-d). These facets were digitized at different spatial scales (Figure 3c), from the smallest scale allowed by the resolution of the data to the largest scale (Figures 3a,b) allowing for geological consistency. For a better statistical representativeness, this test was reproduced on five different areas. The orientation of the largest facet was defined as reference value. The angle calculated between the pole of each facet and the pole of the reference facet was plotted against GQI (Figure 3e). When this angle tends towards 0, the geometric characteristics of the facet are sufficient to reliably measure orientation. The graph shows that the angular differences tend towards 0 for GQI values above 100 or 200 (Figure 3e). To be more inclusive, we set a threshold of 100. Subsequently, data with a GQI < 100 are filtered out. Over the three transects, this GQI resulted in the filtering of 23.4% of the facets digitized in VR and 48.2% of the facets digitized in MM.

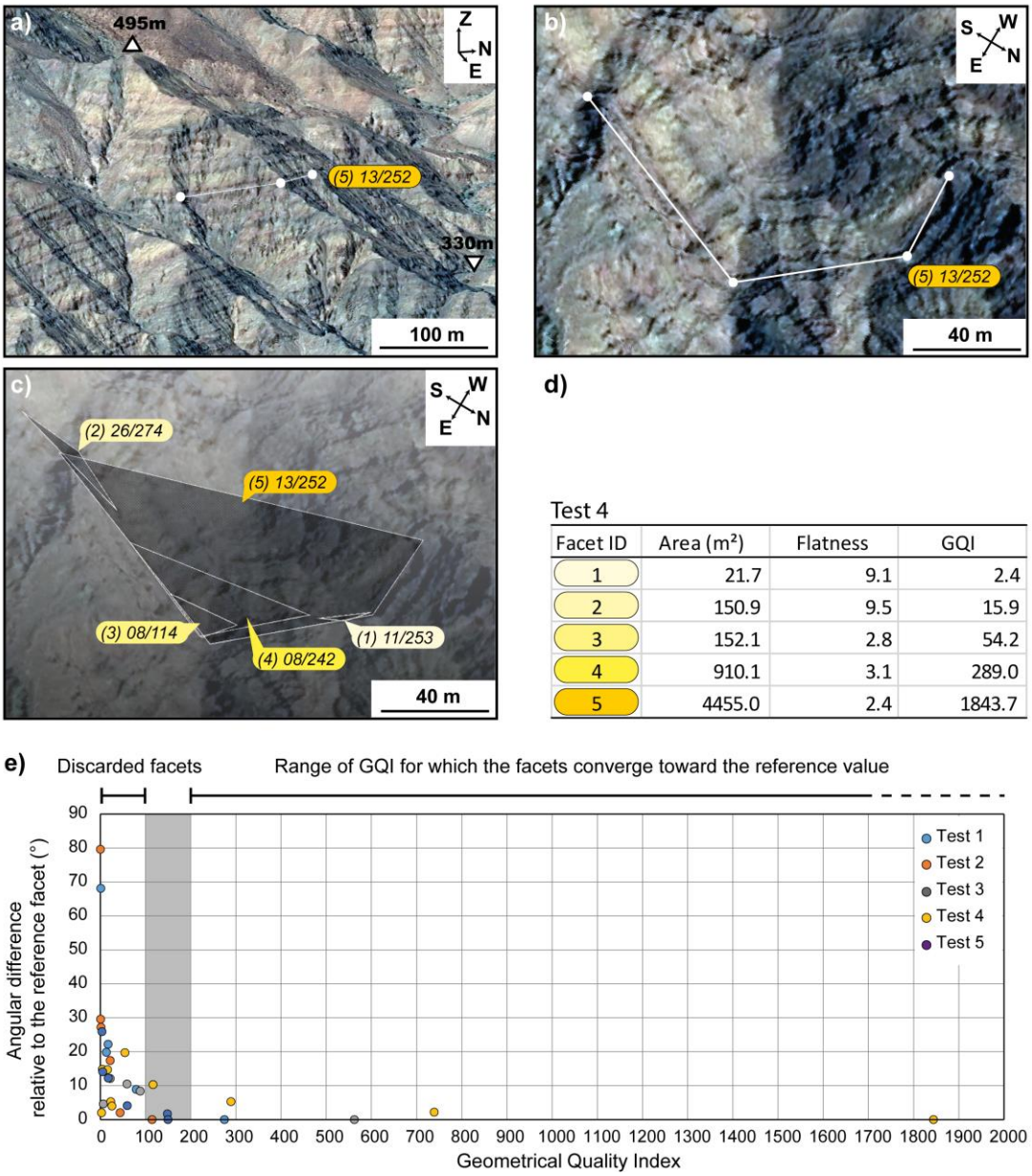

Figure 3. a), b) 3D and top views of the *CloudCompare* digitization of the reference facet (the largest possible on test area 4). The resulting dip and dip direction are displayed in the yellow box. c) Arrangement of digitalized facets at different scales, on the same lava flow, for test area 4. d) Surface area, flatness and GQI values resulting from the different facets in c). Facet 5, with the highest GQI, is the reference facet. e) Plot of the angle calculated between the pole of each measured facet and the pole of the reference facet, as a function of the geometric quality index (GQI). Angle tending towards 0 indicates a GQI sufficient to show a reliable value for facet orientation.

Since a linear least-square method is applied to fit the 3D picking, the related correlation coefficient (R^2) evaluates, a posteriori, the quality of the 3D points alignment along a single facet. The threshold value on the R^2 coefficient was arbitrarily fixed to 0.7, with facets showing a lower

R^2 being excluded from the discussion. Out of the 742 measurements made along the different studied transects, only 5.5% show a very bad R^2 coefficient ranging from 0 to 0.7 and only 17% are below 0.9. Subsequently, data with a $R^2<0.7$ were filtered out.

A flowchart (in supplementary material) summarizes the different processing stages and associated technical constraints.

4. Results and potential for geological interpretation

4.1. Intrinsic quality of facet orientation measurements

We used a statistical approach to assess the accuracy of the method. To do this, we postulated that lava within a limited number of successive flows must have consistent orientations. We thus exploited the possible redundancy of information by picking out as many flows as possible within four different sequences of about 100m in thickness (sampling more than 10 facets), located in distinct areas (Figure 4). The "intra-sequence" dispersion of facets orientation represents an indicator of the accuracy of the method (Table 1). The dispersion in orientation of the facets follows a Fisher distribution, i.e. a circular symmetry around a mean direction. The dispersions we obtain are characterized with high values of the concentration parameter ($300 < \kappa < 2000$) and homogenous values of the radius of the Fisher's confidence cone ($\alpha 95 < 2.1°$, Table 1). The global accuracy of the method is thus estimated to be about 2°.

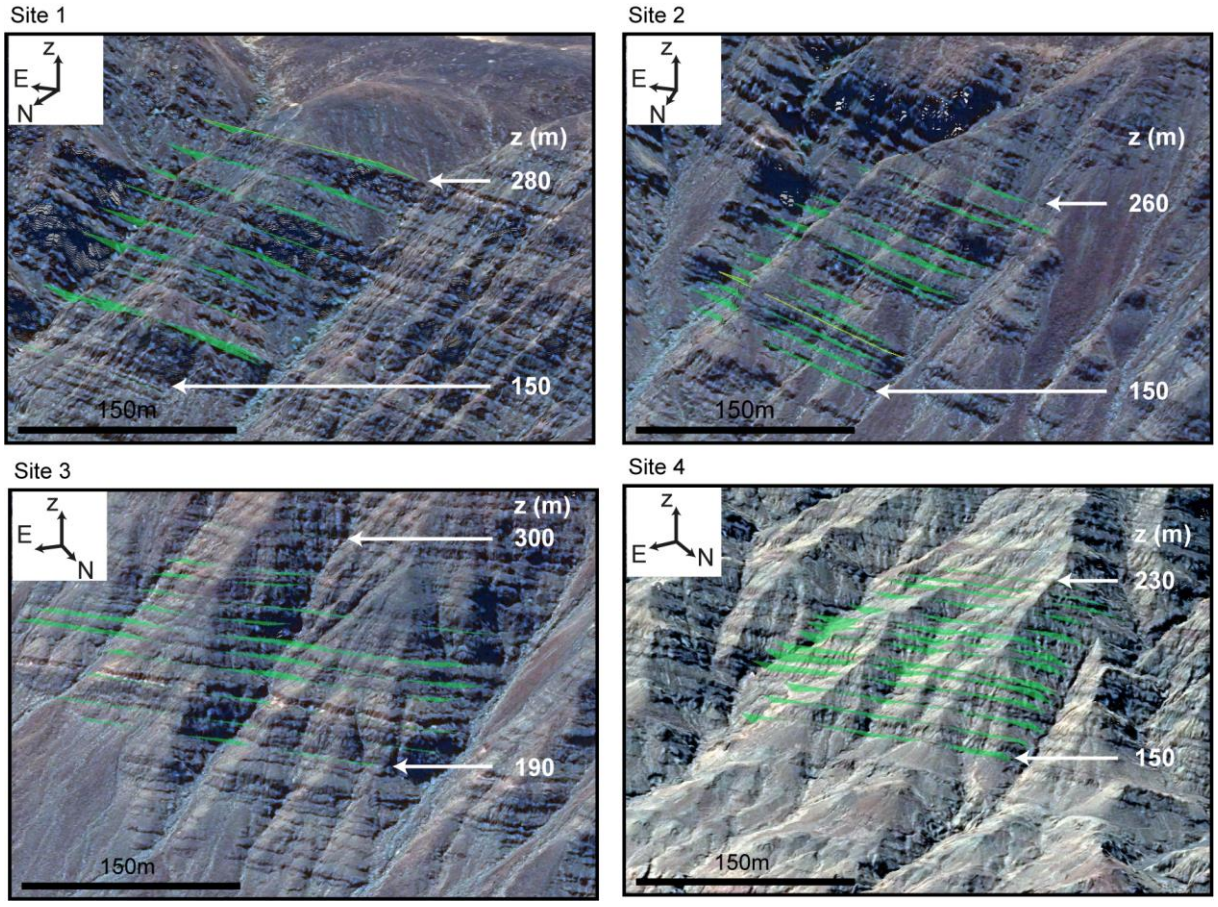

Figure 4. 3D views (from *CloudCompare*®) of sites used to test the “intra-sequence" dispersion of the measured orientations (see Table 1). The greenish virtual planes are those picked in MM.

Table 1. Use of the "intra-sequence" dispersion of orientation measurements as an indicator of the quality of the method.

			Fisher’s statistics	
Lava sequences	Number of facets	Difference of alt. (m)	$\alpha 95$ (°)	κ
1-VR	11	97	1.8	601
1-MM	11	138	1.8	608
2-VR	12	104	1.8	528
2-MM	13	112	0.9	1778
3-VR	10	116	1.2	1571
3-MM	11	118	1.8	527
4-VR	14	79.2	1.9	407
4-MM	14	71	2.1	332

4.2. Inter-comparison of measurements between VR and MM methods

To ensure consistency of the approach, we also compared the two methods. The renderings of the 3D colored point cloud in *CloudCompare*® and the 3D tiled model displayed in the VR application are visually rather different. In *CloudCompare*®, the zoom on the colored point cloud tends to generate a coarse and “pointillist” appearance of the outcrop, whereas the interpolation in VR results in a smoother aspect to the orthoimage (Figures 2c, 2d). As a result, the picked points tend to be at slightly different locations according to the method. As each facet contains the coordinates of its centroid, it is possible to identify facets picked with both methods and located at the same position (here, we set a tolerance radius +/-5 m on the position). In the three transects studied (A, B & C), 74 pairs of facets satisfied this criteria. We calculated, in 3D, the angle between the normals of the facets obtained in VR and MM (Figure 5). The mean difference is about 2.3°, with a standard deviation of 1.6° (Figure 5).

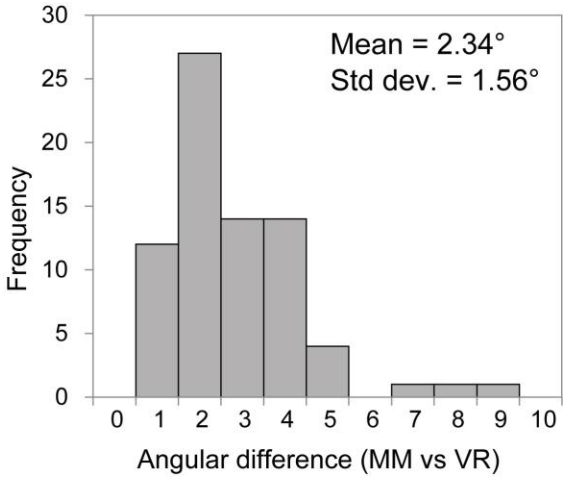

Figure 5. Angular difference between similar pairs of facets (elevation diff. < 5m) measured in Mouse Mode (MM) and Virtual Reality (VR). 74 pairs of corresponding facets were found in the transects A, B & C.

Figure 6 represents the measured dips *versus* dip directions in the three studied transects. The grey points are those that did not pass the quality control ($R^2 < 0.7$ and/or GQI < 100). Overall, the remaining measurements show good intrinsic and inter-method consistency. Nevertheless, there are still some outliers (Figures 6b, 6c), probably due to geologically irrelevant digitization. The facets corresponding to these outliers are then manually removed for geological analysis.

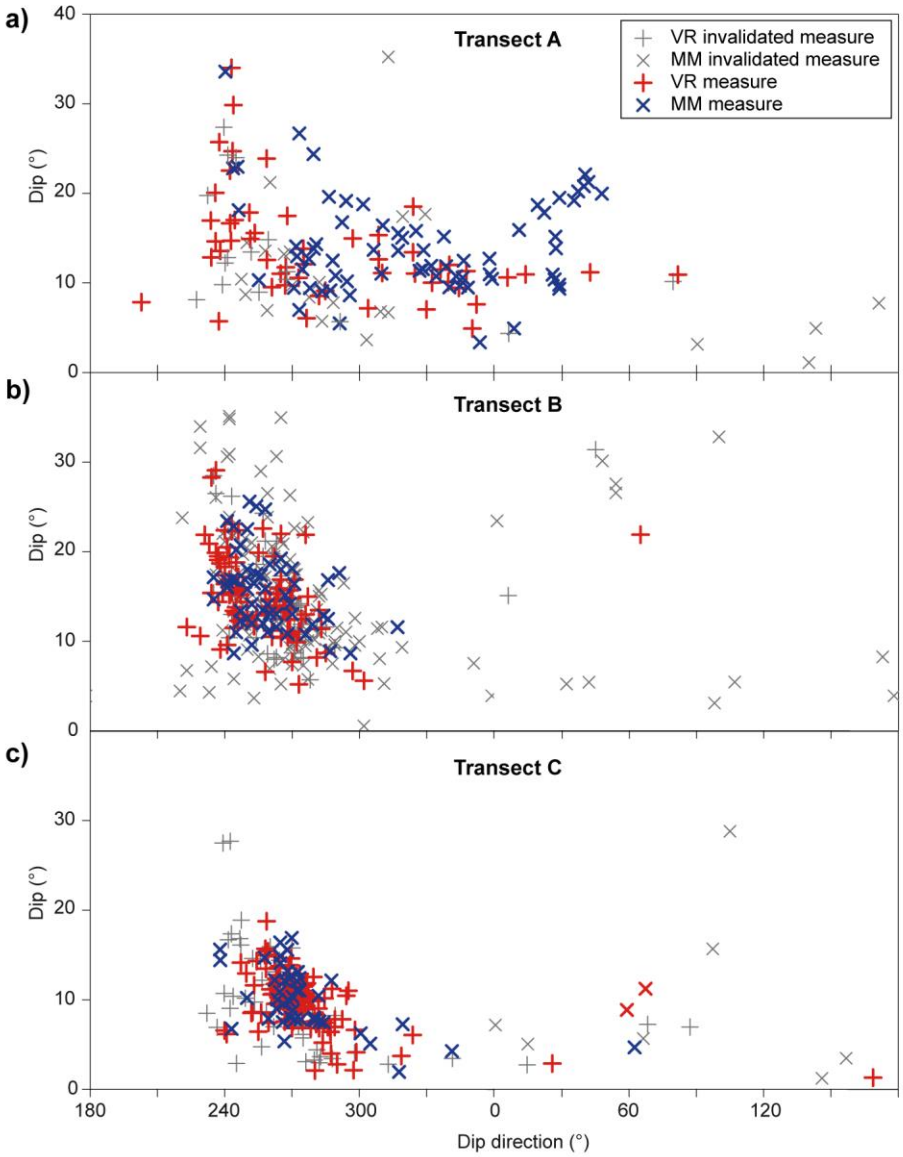

Figure 6. Dip versus dip direction computed from the picked facets for the A (a), B (b) and C (c) transects (see Figure 2a).

4.3. Possible geological interpretation of these measurements

Although the aim of this contribution is not to elaborate on the tectonic implication of those results (see forthcoming contributions based on map-scale analysis using this method), the scientific potential of the method can be illustrated from the data set. The volcanic sequence underlying the Upper Stratoïd Formation (USF) shows significant variations with altitude in strike and dip (Figure 7). However, to determine the attitude of the lavas below the SW-ward dipping Upper Stratoïd Formation (USF, Geoffroy et al., 2014), it is necessary to rotate clockwise (looking NW) the collected data to restore the Upper Stratoïd flows to the horizontal. The strike of the horizontal

rotation axis and the rotation angle were, respectively, the strike and the dip of the USF, as extracted from the Pleiades images (i.e., N130E and 20° respectively, Figure 7a). We hereby illustrate the tectonic information about to be obtained from our results from Transect B (Figure 7). The data rotation leads to a strong modification of the dip direction of the underlying sequence, from an average WSW direction (Figure 7b), toward a N to NNE direction (Figure 7c). Furthermore, after this tilt-correction, the volcanic sequence below the USF shows a clear upward decrease in flow dip (Figure 7c).

To summarize, the data obtained on the Pleiades imagery allow to demonstrate that the USF overlies a fan-like volcanic wedge dipping northward to north-north-eastward (Figure 7c). This striking result confirms that the emplacement of the volcanics older than 2 Ma in the eastern Afar area was syntectonic (Geoffroy et al., 2014).

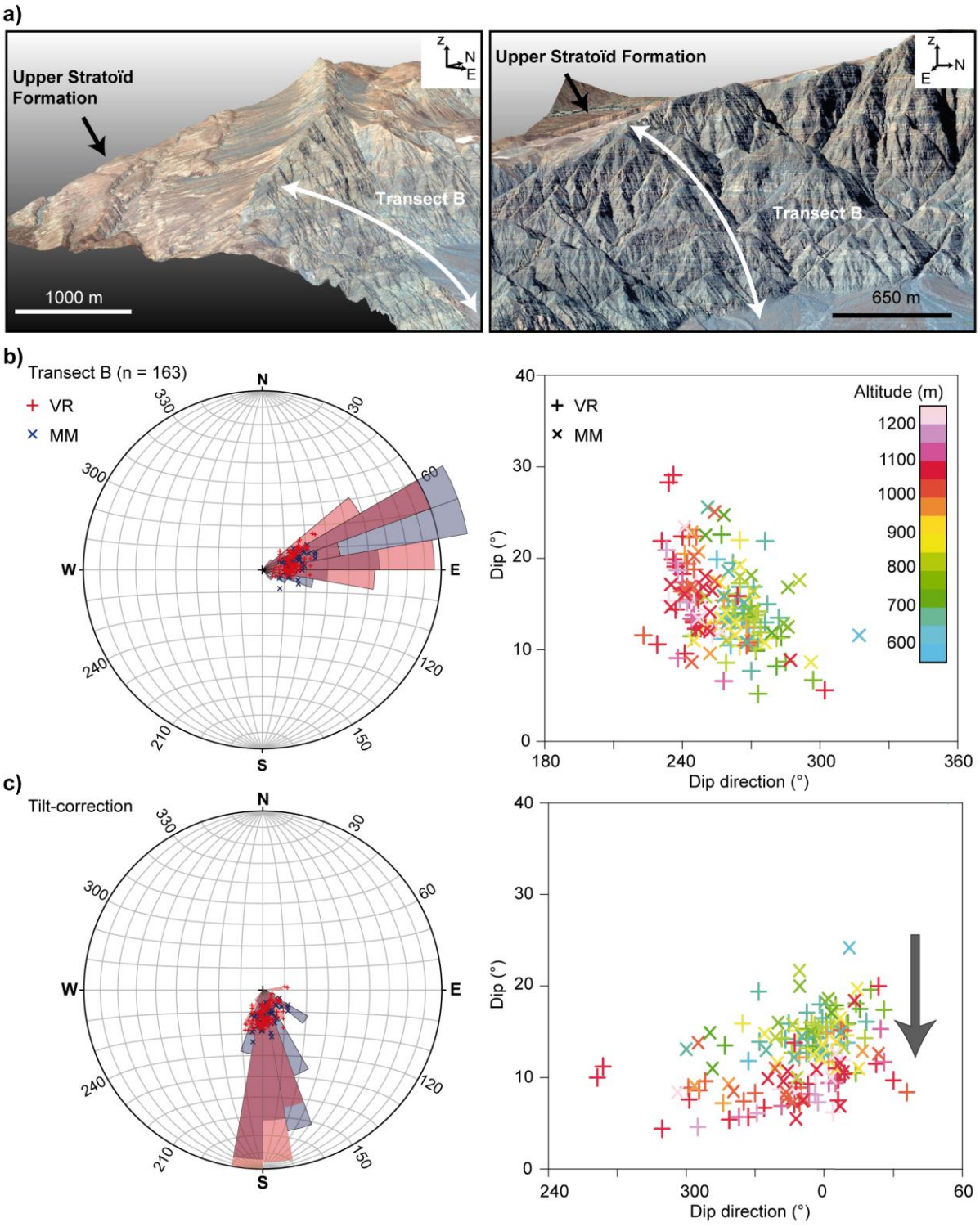

Figure 7. a) Two 3D views, to the NNW (left) and to the W (right), of the surrounding outcrops of Transect B. Note the Upper Stratoïd Formation lava flows exposed on the western flank of the block. Their average strike and dip are N130°E and 20° respectively. b) Transect B related poles of planes and rose diagram of the poles of planes plotted on a lower-hemisphere, equal-area,

stereonet projections (left). The same planes are also plotted on a diagram showing dip versus dip direction variations, with the colour scale for the altitude of the lava flows. c) Same data restored from the SW-tilt of the Upper Stratoïd Formation. Note the outstanding decrease in dip with altitude (grey arrow).

5. Discussion

5.1. Importance of VHR for geological analysis

To avoid biases in geological interpretation of the data, very high resolution of orthoimage and DEM, associated with a quality assessment, is essential. The resolution of the orthoimage ensures good visualisation of the different lava strata and therefore the accuracy of the operator's digitisation of stratum boundaries. The quality of the DEM (resolution and accuracy) ensures that the data exported after digitizing are accurate. Figure 8 presents the order of magnitude of the error in the dip angle estimation, for a given dip direction, provoked by an altitude (Z) error, for different facet sizes.

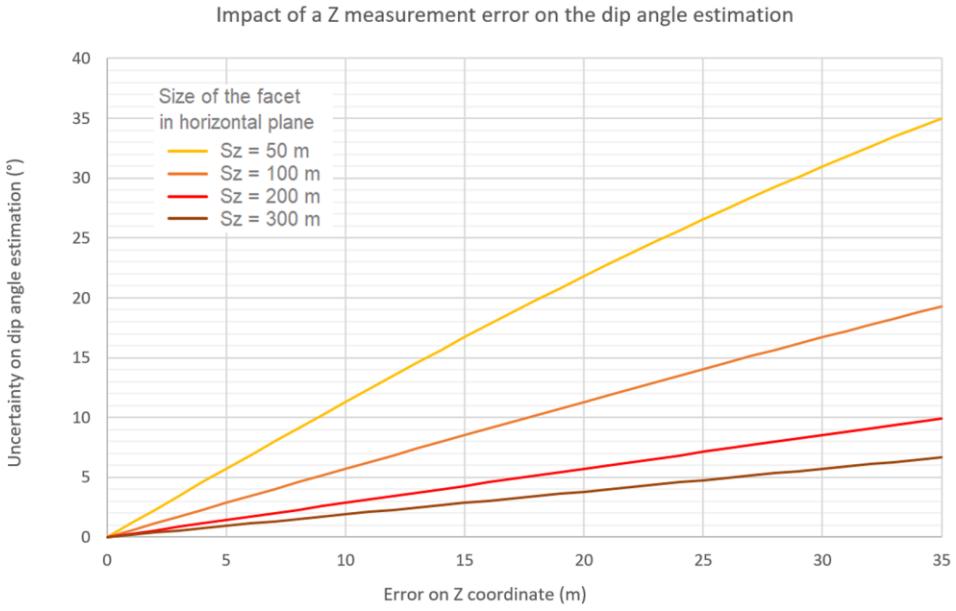

Figure 8. Error in dip angle (for a given dip direction) as a function of errors in altitude (Z) and horizontal length of the facet.

For a given DEM, it is preferable to consider large facets to limit the impact of any error in altitude. In the present study, apart from local artefacts, the Pleiades DEM has a sub-meter accuracy, and the horizontal extent of the facets is about 40 to 300 m, which corresponds to errors in dip measurements less than, or equal to, +/-2°.

Considering the updating frequency and the image quality, Google Earth® can be very useful to pre-identify areas of interest. Nevertheless, users should keep in mind that the related DEM does not have such a high resolution (a priori, 30 m for our study area - https://explorer.earthengine.google.com/#detail/USGS%2FSRTMGL1_003), involving uncertainty in the position of picked points. Using a DEM with 30-m resolution was a source of erroneous measurements of dip directions in previous studies. To assess the differences between point picking in Google Earth® and on the Pleiades DEM, three vectors were defined along lava flow limits (Figure 9). Considering vectors, we did not take into account absolute errors in georeferencing, but only the impact of the DEM resolution in data consistency. The gaps in the vertical components of the vectors are given in Table 3. These gaps are variable in direction and intensity depending on the location, being a priori more greatly increased on sharp edges or narrow concavities, where the topography is smoothed by low resolution. Varying from 12.4 m to -34.5 m (for horizontal vector sizes of 120.4 m and 92.2 m, respectively), according to the graph in Figure 8, these gaps would induce an error between around 5° and 21° in the dip angle estimation.

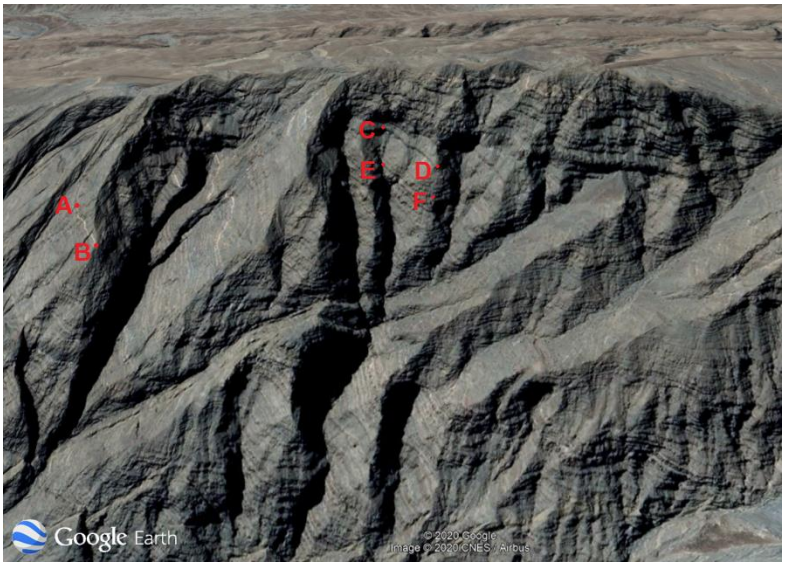

Figure 9: Positions of the vector extremities used to compare Google Earth® point picking and Pleiades DEM point picking.

Table 3: Comparison of the vertical components (Z) of the vectors (Figure 10) picked in Google Earth® and on the Pleiades DEM.

	Size of the vector in the horizontal plane	*Z_{GE} component of the vector on Google Earth*	*$Z_{Pleiades}$ component of the vector on Pleiades DEM*	*Gap between Z_{GE} and $Z_{Pleiades}$*
$\overrightarrow{AB}$	120.4 m	-20 m	-32.3 m	12.4 m (38.2%)
$\overrightarrow{CD}$	101.4 m	-46 m	-13.4 m	-32.6 m (242.1%)
$\overrightarrow{EF}$	92.2 m	-38 m	-3.5 m	-34.5 m (979.5%)

5.2. Mouse Mode and Virtual Reality comparison

Some criteria of comparison between MM and VR are summarized in Table 4. With the VR application, the operator is immersed in a virtual environment where he/she can easily travel over the study area, making measurements over hundreds of kilometers, combining the aerial synoptic view and ground-level view. As a consequence, the number of facets picked was around 30% higher in VR than in MM. Furthermore, quality control by GQI results in twice as many facets being filtered in MM as in VR (48.2% rejected in MM versus 23.4% rejected in VR), which suggests that VR helps the operator to digitize more reliable facets (geometrically speaking).

Table 4. Overall comparison of Mouse Mode (MM) and Virtual Reality (VR) approaches.

	MM approach	VR approach
Software developments	Use of free existing software tools	Development of the VR apps + dedicated accessories (≈ several k€)
Ergonomics	Pre-extraction of the transect	Fluidity of displacement across the area
Visual aspect of the 3D datasets	satisfactory	highly satisfactory
Time needed for picking virtual facets in a transect (e.g. transect B)	~ 6 h	~ 2.5 h
Difficulty of the point picking for the operator	Arduous and long	Easy and recreational
Number of picked facets per transect	~ 60-80	~ 100-120
Uncertainty in 3D orientation (Fisher's distribution)	$\alpha 95$: Mean = 1.65°	$\alpha 95$: Mean = 1.675°
Percentage of facets rejected at quality control (R^2 + GQI)	28.3 %	54.4 %

VR has a high potential to enhance the visual impact of a complex geological context and to improve interpretation of the geological processes shaping a study area. Furthermore, it also offers great future possibilities for education. In geoscience education, the value of field trips is undisputed, contributing to fostering both field experience and community learning. Nevertheless, immersive technologies can improve accessibility to some areas and offers the opportunity to better prepare field trips beforehand and to complete field observations or process them in depth afterwards. With such innovative teaching, students are not limited to passive viewing of content as this immersive active learning increases their involvement (Boniello et al., 2019; Klippel et al., 2019). When given the opportunity and tools to develop a sense of place in the local and regional environment, as VR does, students improve their conceptual knowledge and ability to assemble key concepts and to apply critical thinking skills (Monet and Greene, 2012). In addition, as

mentioned in Boniello et al. (2019), these VR approaches contribute to increasing interest among a new generation of students who are already used to interacting with these new tools. The development of a VR tool able to load new datasets on the fly and in virtual reality could be a good investment to enrich the results of field surveys.

6. Conclusion

Facet 3D orientation is a simple but essential parameter for any geological interpretation whatever the geological context, in terrestrial planets. VHR remote sensing methods, such as stereo restitution from Pleiades imagery, offer the opportunity to retrieve the spatial position and the characteristics of geologic layers. After a quality control to assess the geometric relevance of the digitization, both the MM and VR methods give reliable results within about 1° to 3°. As they allow a synoptic coverage of large areas, such remote sensing approaches complement or may even replace traditional field techniques, especially in such a setting of lava piles.

To investigate Pleiades imagery, VR enables the operator to immerse themselves in a very realistic virtual environment and to easily make measurements over hundreds of kilometers, combining both an aerial synoptic view and a ground-level view. Such immersive tools clearly present great potential for geoscience, particularly in environments that are difficult to access because they suffer from political problems, inaccessible terrain, or are underwater or in extra-terrestrial environments..

Acknowledgments

The Pleiades images used in this study were ordered as part of the ISIS program of the CNES (French National Centre for Space Studies) and provided by DataTerra via the DINAMIS platform. The images can be consulted on the Airbus Geostore catalogue: https://www.intelligence-airbusds.com/en/4871-geostore-ordering. The identifiers of our images are: PHR1B_201811090748221_FR1_PX_E042N11_0517_01013;
PHR1A_201811100740439_FR1_PX_E042N11_0520_01787;
PHR1B_201811230740421_FR1_PX_E042N11_0524_01787;
PHR1B_201812120744316_FR1_PX_E042N11_0417_00822;
PHR1B_201812190740409_FR1_PX_E042N11_0320_01787;
PHR1A_201812250744194_FR1_PX_E042N11_0324_01804.

References

Bagnardi, M., González, P.J., Hooper, A., 2016. High-Resolution Digital Elevation Model from Tri-Stereo Pleiades-1 Satellite Imagery for Lava Flow Volume Estimates at Fogo Volcano. Geophysical Research Letters 43(12), 6267-6275. https://doi.org/10.1002/2016GL069457.

Berthier, E., Vincent, C., Magnússon, E., Gunnlaugsson, Á.Þ., Pitte, P., Le Meur, E., Masiokas, M., Ruiz, L., Pálsson, F., Belart, J.M.C., Wagnon, P., 2014. Glacier Topography and

Elevation Changes Derived from Pléiades Sub-Meter Stereo Images. The Cryosphere 8(6), 2275-91. https://doi.org/10.5194/tc-8-2275-2014.

Beyer, R. A., Alexandrov, O., McMichael, S., 2018. The Ames Stereo Pipeline: NASA's Open Source Software for Deriving and Processing Terrain Data. Earth and Space Science 5(9), 537-48. https://doi.org/10.1029/2018EA000409.

Bilotti, F., Shaw, J.H., Brennan, P.A., 2000. Quantitative Structural Analysis with Stereoscopic Remote Sensing Imagery. *AAPG Bulletin*, 84. https://doi.org/10.1306/A96733D8-1738-11D7-8645000102C1865D

Boniello, A., Paris, E., Santoianni, F., 2019. Virtual Reality in Education: Breakthroughs in Research and Practice, in IGI Global (Ed.), Advances in Game-based Learning. https://doi.org/10.4018/978-1-5225-8179-6.

Cattin, R., Doubre, C., De Chabalier, J.-B., King, G., Vigny, C., Avouac, J.-P., Ruegg, J.-C., 2005. Numerical modelling of quaternary deformation and post-rifting displacement in the Asal–Ghoubbet rift (Djibouti, Africa). Earth and Planetary Science Letters 239(3), 352–367.

Chauvet, F., Geoffroy, L., Guillou, H., Maury, R. C., Le Gall, B., Agranier, A., Viana, A., 2019. Eocene Continental Breakup in Baffin Bay. Tectonophysics. 757, 170-186. https://doi.org/10.1016/j.tecto.2019.03.003.

Checa, D., Bustillo, A., 2020. A Review of Immersive Virtual Reality Serious Games to Enhance Learning and Training. Multimedia Tools and Applications 79, 5501-5527. https://doi.org/10.1007/s11042-019-08348-9.

Chenrai, P., Jitmahantakul, S., 2019. Applying Virtual Reality Technology to Geoscience Classroom. Review of International Geographical Education Online. https://doi.org/10.33403/rigeo.592771.

Civet, F., Le Mouélic, S., 2015. VR-Planets: A 3D immersive application for real-time flythrough images of planetary surfaces. Proceeding of the 17th EGU General Assembly Conference, Vienna, Austria.

Collin, A., Hench, J. L., Pastol, Y., Planes, S., Thiault, L., Schmitt, R. J., Holbrook, S.J., Davies, N., Troyer, M., 2018. High Resolution Topobathymetry Using a Pleiades-1 Triplet: Moorea Island in 3D. Remote Sensing of Environment 208, 109-119. https://doi.org/10.1016/j.rse.2018.02.015.

Cozzi, P., Ring, K., 2011. 3D engine design for virtual globes. A.K. Peters (Ed.), CRC Press.

Doubre, C., Manighetti, I., Dorbath, L., Dorbath, C., Bertil, D., Delmond, J., 2007. Crustal structure and magmato-tectonic processes in an active rift (Asal-Ghoubbet, Afar, East Africa): 2. Insights from the 23-year recording of seismicity since the last rifting event. Journal of Geophysical Research. 112, B05406. https://doi.org/10.1029/2006JB004333.

Gasse, F., Dagain, J., Fournier, M., Mazet, G., Richard, O., 1987. Geological Map of the Republic of Djibouti. ORSTOM, Paris, sheet Dikhil, scale 1:100000.

Geoffroy, L., 2005. Volcanic Passive Margins. Comptes Rendus Geoscience 337(16), 1395-1408. https://doi.org/10.1016/j.crte.2005.10.006.

Geoffroy, L., Le Gall, B., Daoud, M., Jalludin, M., 2014. Flip-flop detachment tectonics at nascent passive margins in SE Afar. Journal of the Geological Society of London 171(5), 689-694. http://dx.doi.org/10.1144/jgs2013-135.

Kidane, T., Courtillot, V., Manighetti, I., Audin, L., Lahitte, P., Quidelleur, X., Gillot, P.-Y., Gallet, Y., Carlut, J., Haile, T., 2003. New paleomagnetic and geochronologic results from Ethiopian Afar: Block rotations linked to rift overlap and propagation and determination of a ~2 Ma reference pole for stable Africa. Journal of Geophysical Research: Solid Earth 108. https://doi.org/10.1029/2001JB000645

Klippel, A., Zhao, J., Jackson, K.L., La Femina, P., Stubbs, C., Wetzel, R., Blair, J., Wallgrün, J.O., Oprean, D., 2019. Transforming Earth Science Education Through Immersive Experiences: Delivering on a Long Held Promise. Journal of Educational Computing Research 57, 1745–1771. https://doi.org/10.1177/0735633119854025

Lahitte, P., Gillot, P.-Y., Kidane, T., Courtillot, V., Bekele, A., 2003. New age constraints on the timing of volcanism in central Afar, in the presence of propagating rifts. Journal of Geophysical Research: Solid Earth 108. https://doi.org/10.1029/2001JB001689

Le Gall, B., Daoud, M.A., Maury, R., Gasse, F., Rolet, J., Jalludin, M., Caminiti, A.M., Moussa, N., 2015. Geological Map of the Republic of Djibouti (1st edition). Centre d'Etude et de Recherche de Djibouti (CERD) and CCGM, scale 1:200 000.

Le Mouélic, S., L'Haridon, J., Civet, F., Mangold, N., Triantafyllou, A., Massé, M., Le Menn, E., Beaunay, S., 2018. Using virtual reality to investigate geological outcrops on planetary surfaces. Proceedings of the 20th EGU General Assembly Conference, Vienna, Austria, 2018.

Letortu, P., Jaud, M., Théry, C., Nabucet, J., Taouki, R., Passot, S., Augereau, E., 2020. The Potential of Pléiades Images with High Angle of Incidence for Reconstructing the Coastal Cliff Face in Normandy (France). International Journal of Applied Earth Observation and Geoinformation 84, 101976. https://doi.org/10.1016/j.jag.2019.101976.

Manighetti, I., Tapponnier, P., Gillot, P., Jacques, E., Courtillot, V., Armijo, R., Ruegg, J.C., King, G., 1998. Propagation of rifting along the Arabia-Somalia plate boundary: Into Afar. Journal of Geophysical Research 103(B3), 4947–4974.

Massironi, M., Baggio, P., Dal Piaz, G.V., Loizzo, R. "Brittle tectonics in the northwestern Alps: remote sensing applications". In Proc. Vol. 3222, Earth Surface Remote Sensing, pp. 329 39, Aerospace Remote Sensing '97, 1997, London, United Kingdom, 1997. https://doi.org/10.1117/12.298158.

Monet, J., Greene, T., 2012. Using Google Earth and Satellite Imagery to Foster Place-Based Teaching in an Introductory Physical Geology Course. Journal of Geoscience Education 60, 10–20. https://doi.org/10.5408/10-203.1

Moysey, S.M.J., Lazar, K.B, 2019. Using Virtual Reality as a Tool for Field-Based Learning in the Earth Sciences. In: Lansiquot, R.D., MacDonald, S.P. (Eds), Interdisciplinary Perspectives on Virtual Place-Based Learning, Springer International Publishing. https://doi.org/10.1007/978-3-030-32471-1_7.

Nelson, C.E., Jerram, D.A., Hobbs, R.W., Terrington, R., Kessler, H., 2011. Reconstructing flood basalt lava flows in three dimensions using terrestrial laser scanning. Geosphere 7, 87–96. https://doi.org/10.1130/GES00582.1

Nishidai, T., Berry, J.L., 1990. Structure and hydrocarbon potential of the Tarim Basin (NW China) from satellite imagery. *Journal of Petroleum Geology*, 13(1), 35-58. https://doi.org/10.1111/j.1747-5457.1990.tb00250.x.

Pedersen, A.K., Watt, M., Watt, W.S., Larsen, L.M., 1997. Structure and stratigraphy of the Early Tertiary basalts of the Blosseville Kyst, East Greenland. Journal of the Geological Society 154, 565–570. https://doi.org/10.1144/gsjgs.154.3.0565

Perko, R., Raggam, H., Gutjahr, K., Schardt, M., 2014. Assessment of the Mapping Potential of Pléiades Stereo and Triplet Data. ISPRS Annals of Photogrammetry, Remote Sensing and Spatial Information Sciences, II-3, 103-9. https://doi.org/10.5194/isprsannals-II-3-103-2014.

Poli, D., Remondino, F., Angiuli, E., Agugiaro, G., 2015. Radiometric and Geometric Evaluation of GeoEye-1, WorldView-2 and Pléiades-1A Stereo Images for 3D Information Extraction. ISPRS Journal of Photogrammetry and Remote Sensing 100, 35-47. https://doi.org/10.1016/j.isprsjprs.2014.04.007.

Riisager, J., Riisager, P., Pedersen, A.K., 2003. Paleomagnetism of large igneous provinces: case-study from West Greenland, North Atlantic igneous province. Earth and Planetary Science Letters 214, 409–425. https://doi.org/10.1016/S0012-821X(03)00367-4

Shean, D. E., Alexandrov, O., Moratto, Z., Smith, B.E., Joughin, I.R., Porter, C., Morin, P., 2016. An automated, open-source pipeline for mass production of digital elevation models (DEMs) from very high-resolution commercial stereo satellite imagery. ISPRS Journal of Photogrammetry and Remote Sensing 116, 101-117. https://doi.org/10.1016/j.isprsjprs.2016.03.012

Stumpf, A., Malet, J.-P., Allemand, P., Ulrich, P., 2014. Surface Reconstruction and Landslide Displacement Measurements with Pléiades Satellite Images. ISPRS Journal of Photogrammetry and Remote Sensing 95, 1-12. https://doi.org/10.1016/j.isprsjprs.2014.05.008.

Zhou, Y., Parsons, B., Elliott, J.R, Barisin, I., Walker, R.T., 2015. Assessing the Ability of Pleiades Stereo Imagery to Determine Height Changes in Earthquakes: A Case Study for the El Mayor-Cucapah Epicentral Area. Journal of Geophysical Research: Solid Earth 120(12), 8793-8808. https://doi.org/10.1002/2015JB012358.

Supplementary material

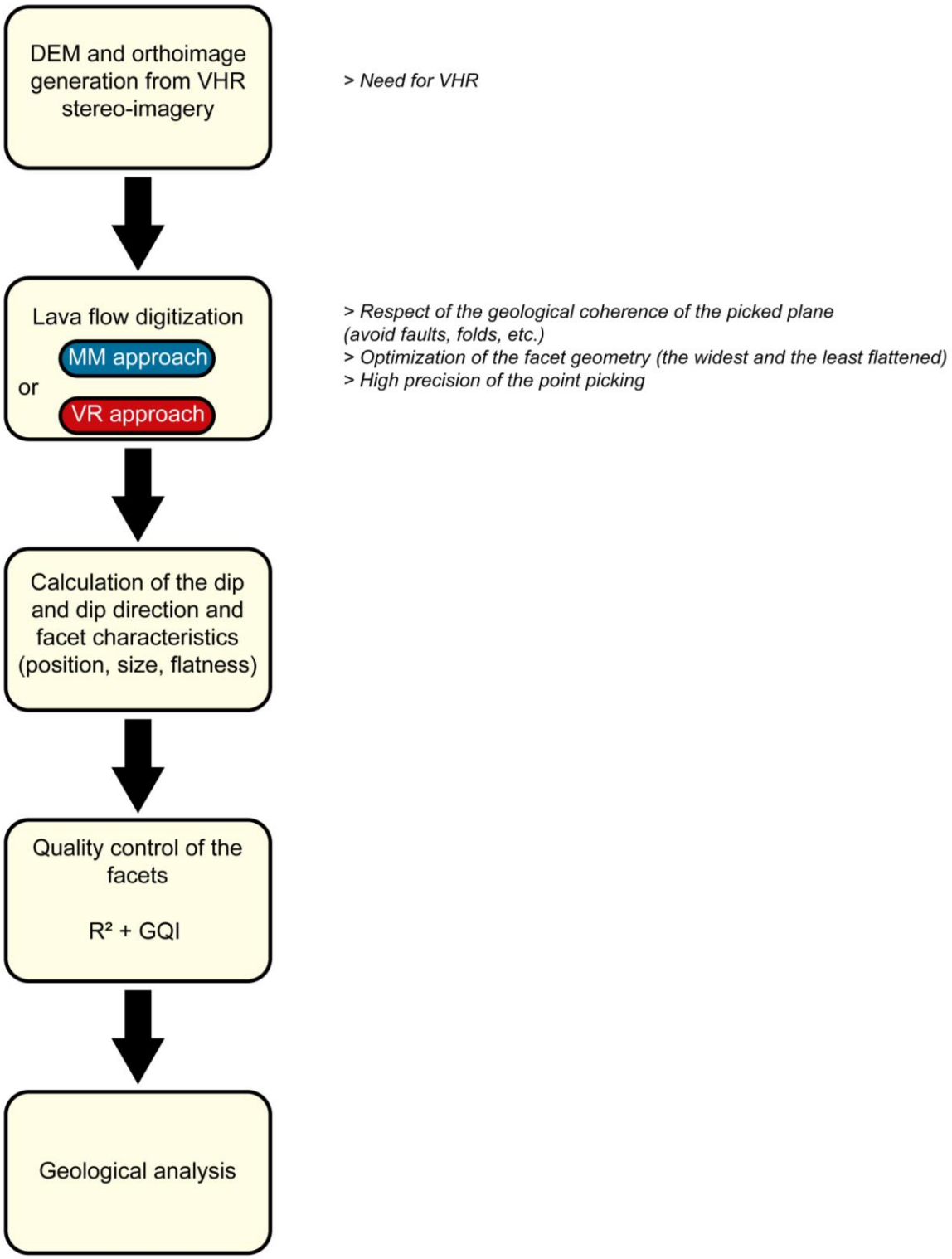

Sup. Mat. Flowchart (left) and related technical considerations (right) for each step.